Available online at www.sciencedirect.com
ScienceDirect
International Journal of Thermal Sciences 48 (2009) 449–460
International Journal of Thermal Sciences
www.elsevier.com/locate/ijts

Prediction of micro-explosion delay of emulsified fuel droplets

D. Tarlet [a], J. Bellettre [b,*], M. Tazerout [c], C. Rahmouni [a]

[a] *CREED (Veolia Environnement), 291 Av. Dreyfous Ducas, 71520 Limay, France*
[b] *Laboratoire de Thermocinétique UMR 6607 CNRS – Université de Nantes, rue Christian Pauc, B.P. 50609, 44306 Nantes Cedex 3, France*
[c] *GEPEA UMR 6144 CNRS, Ecole des Mines de Nantes, ENITIAA – Université de Nantes, 4, rue Alfred Kastler, B.P. 20722, 44307 Nantes Cedex 3, France*

Received 30 November 2006; received in revised form 15 February 2008; accepted 12 May 2008

Available online 18 June 2008

Abstract

Burning a water-in-oil emulsion enables reduction in solid and gaseous pollutants in comparison with neat oil. In the emulsion, Heavy Fuel-Oil and water lie in distinct phases, having a high difference in boiling point (up to 200 K). In an emulsion droplet injected and subsequently heated inside a flame, the internal water droplets are enclosed inside the emulsion and do not systematically vaporise at boiling point. They are known to reach a metastable state, breaking up at a temperature below the spinodal limit of water. From this moment, the surrounding Fuel-Oil is fragmented into numerous faster and smaller droplets by the suddenly expanding steam. This physical phenomenon is called "micro-explosion". This work demonstrates a numerical modelisation of unsteady heat and mass transfer at the surface and inside of the emulsion droplet, and provides a prediction of its micro-explosion delay, using homogeneous nucleation hypothesis. This assumption of homogeneous nucleation for internal water droplets matches the use of a "drop tower" experimental facility. Finally, comparisons between predicted ranges for micro-explosion delays and experimental delays from literature are discussed, along with combustion parameters (ambient temperature, relative velocity) and combustible emulsion parameters. As a result, the experimental and numerical micro-explosion delays decrease with liquid or ambient temperature and relative velocity, and increase with water content and radius of emulsion droplet. Their low average deviation reveals the accuracy of the assumption of homogeneous nucleation in the considered situations.

Keywords: Micro-explosion delay; Emulsion droplet; Drop tower; Homogeneous nucleation; Heavy Fuel-Oil

1. Introduction

Micro-explosion of emulsified fuel droplets has been extensively studied as a mean to improve combustion characteristics and emissions of burning sprays. With emulsion-burning sprays, emission of pollutants such as carbonaceous residues [1,2] and NO_x [3] are lowered in comparison with pure Heavy Fuel-Oil. Solid and gaseous pollutants are crucial matters concerning viscous fuels, such as residual oil or valorized animal fat, although these fuels are not directly addressed in this paper. These fuels are usually burnt as a complement to natural gas in heating devices.

Instead of a neat fuel droplet, an emulsified one is injected into a flame, undergoing an intense heat transfer. Its internal water droplets, that are enclosed inside the emulsion, do not systematically vaporise at boiling point [4]. They reach a liquid metastable state which is known to break up at a temperature between the boiling point and the well-known spinodal limit of water. The sudden and dramatic expansion of vaporising water leads to disintegration of the whole emulsion droplet. Indeed, the emulsified fuel-oil (with boiling point up to 650 K) is still liquid when fragmented into smaller droplets by expansion of vaporising water. Micro-explosion is then supposed to be extremely fast, leading to disintegration of whole parts, or totality of the emulsion droplet [5]. The underlying hypothesis is the launching of nucleation on a water droplet when in contact with steam of the vaporising nearest one [6]. A consequence of that is a unique and total disintegration of the emulsion droplet generally observed with water droplets dispersed finely and uniformly enough inside the emulsion [7]. The characteristic duration of such a disintegration is cited as less than 0.2 ms [6,8].

* Corresponding author. Tel.: (+ 33)2 40 68 31 33; fax: (+33)2 40 68 31 41.
E-mail address: jerome.bellettre@univ-nantes.fr (J. Bellettre).

1290-0729/$ – see front matter
doi:10.1016/j.ijthermalsci.2008.05.005

Nomenclature

c_p	specific heat	$J\,kg^{-1}\,K^{-1}$
C	concentration	$kmole\,m^{-3}$
dm	mass of vaporized liquid	kg
dr	thickness of spherical layer	m
f	weight fraction of water in emulsion	
K	mass transfer coefficient	$m\,s^{-1}$
k_C	mass diffusion coefficient	$m^2\,s^{-1}$
L	latent heat	$J\,kg^{-1}$
l	fuel spherical layer	
M	molar mass	$kg\,kmole^{-1}$
m	mass	kg
N	number of internal water droplets	
Nu	Nusselt number	
P	pressure	Pa
Pr	Prandtl number	
Q	heat flux	W
R	ideal gas constant	$J\,kmole^{-1}\,K^{-1}$
Re	Reynolds number	
r	radius	m
S	surface area outside a sphere layer	m^2
Sc	Schmidt number	
T	temperature	K
t	time	s
V	volume	m^3
W	vaporisation flux	$kg\,s^{-1}$
Y	mass fraction	

Greek symbols

β	layer depletion factor	
α	convective coefficient	$W\,m^{-2}\,K^{-1}$
λ	thermal conductivity	$W\,m^{-1}\,K^{-1}$
ρ	density	$kg\,m^{-3}$

Subscripts

air	air
bp	boiling point
CH	hydrocarbon fuel
d	emulsion droplet
ext	superficial layer
film	film
G	gaseous environment
l	fuel spherical layer
p	emulsion droplet
steam	steam
vap	fuel vapor
∞	away in the gaseous phase
w	water

Among combusting sprays, this disintegration into smaller – and faster – droplets of pure Heavy Fuel-Oil is called the second atomization. In comparison with a combusting spray of pure Heavy Fuel-Oil, an example of subsequent decrease in the Sauter Mean Diameter is 50%, enabling a larger interface area between air and fuel, and a better mixing in combustion chambers [9]. Beside this, the presence of water enables a lower flame temperature [10]. Subsequent reductions in emission of pollutants (carbonaceous residues and NO_x) have been extensively studied [1–3,9].

To ensure the occurrence of micro-explosion without considering yet the micro-explosion delay, Law [11] investigates the theoretical influence of parameters such as environment pressure or fuel molar volume on the spinodal limit of water. Using nucleation theory, Wei Biao Fu [4] gives a criterion for the occurrence of micro-explosion based on the size of the emulsion droplet and its volume fraction of water, supposing the formation of a membrane of pure fuel. He also formulates a potential strength for micro-explosion, showing optimums with water fraction and radius of internal water droplets. Chen and Wang [12] investigate combustion characteristics of water-in-oil emulsion droplets, such as ignition delay or burning rates.

The present work aims at introducing a model predicting the micro-explosion delay. It focuses on an unsteady modelisation of heat transfer at the surface and inside an emulsion droplet. The individual emulsion droplet is divided into concentric spherical layers. Physical phenomena such as vaporisation of the emulsion, and influence of gaseous environment temperature and velocity on heat and mass transfers are taken into account and separately validated. As they are calculated together in the sphere layers model, the increase in temperature of internal water droplets is tracked through the time. As the hypothesis of homogeneous nucleation is considered, liquid metastable water approaching its spinodal limit temperature constitutes an upper boundary for the micro-explosion delay. Hence, the micro-explosion delay can be predicted. And supposing that there is no spray collision, or site for heterogeneous nucleation (for instance, a thermocouple in suspended-droplet experiments [13]) means that homogeneous nucleation of water droplets has to be considered. The use of a "drop-tower" facility, where solid surfaces inducing heterogeneous nucleation in the emulsion are absent, and the comparison with results from this model enables to investigate whether the assumption of homogeneous nucleation is relevant or not. As explained by Law [11], the spinodal limit temperature of water (between 550 and 600 K) is used as an upper approximation to predict the onset of homogeneous nucleation.

In the present work, validations of micro-explosion delay are realized under the assumption of homogeneous nucleation using micro-explosion delay measurements by Gollahalli [13] in a "drop-tower" combustion facility. Comparisons between numerical predictions and experimental results are performed, examining 27 different cases. Governing trends in the micro-explosion delay along combustion parameters like water droplet radius or environment temperature are discussed.

Table 1
Thermo-physical properties of Heavy Fuel-Oil

Thermo-physical property	Value used in simulations
Liquid Heavy Fuel-Oil (between 300 K and 600 K)	
Latent heat L_f [J kg^{-1}]	[2.45×10^5; 2.54×10^5]
Heat capacity [J K^{-1} m^{-3}]	[1.9×10^6; 2.1×10^6]
Thermal conductivity [W m^{-1} K^{-1}]	[0.14; 0.15]
Density [kg m^{-3}]	[792; 936]
Vapors of Heavy Fuel-Oil (between 500 K and 1500 K)	
Binary diffusion coefficient [m^2 s^{-1}]	[1×10^{-5}; 9×10^{-5}]
Thermal conductivity [W m^{-1} K^{-1}]	[0.04; 0.12]
Dynamic viscosity [kg m^{-1} s^{-1}]	[1×10^{-5}; 2.8×10^{-5}]

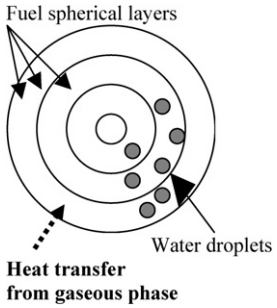

Fig. 1. Principle of the sphere layers model.

2. The sphere layers model

A discretization into concentric spherical layers is adopted in order to model the heat and mass transfer phenomena at the surface and inside the emulsion droplet. In this model, conductive heat transfer is modeled between spherical layers of Heavy Fuel-Oil, and towards their internal water droplets. Table 1 provides the thermo-physical properties of the fuel and the gaseous phase implemented as temperature-dependent. Only constant atmospheric pressure is considered, as required in the further validation cases.

Fig. 1 shows the dispersed phase inserted as numerous spheres of water subtracting volume and showing surface for heat transfer within each spherical layer of fuel. These volumes and surfaces are re-calculated at every step of time, taking into account the thermal expansions of fuel and water. The number of water droplets is assumed to maintain the mass fraction of water as a constant in each spherical layer of the whole emulsion droplet. Finally, water droplets are assumed to be all the same initial radius r_w, and their temperature is considered as homogeneous.

2.1. Governing equations

Eq. (1) is the calculation of heat balance for a sphere layer indiced as l, considering conductive heat transfer from its close layers $l+1$ and $l-1$. Eq. (2) expresses the heat transfer to its internal water droplets Q_l. The l indice increases from the centre ($l = 1$) to the surface of the emulsion droplet ($l = \text{ext}$). Eq. (1) is calculated for each spherical layer of Heavy Fuel-Oil, from the centre to the one just under the superficial one ($l = \text{ext} - 1$).

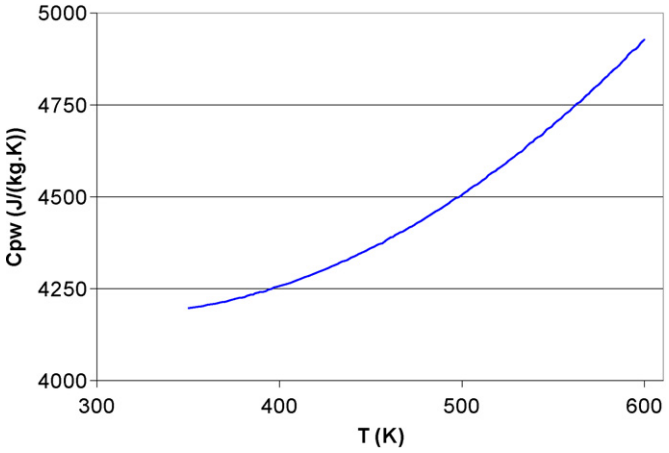

Fig. 2. Specific heat of water – metastable domain by Cahn [15].

The expansion of fuel and water is taken into account through a linear dependence of fuel and water densities to temperature, so diameters of every spherical layer and internal water droplet are calculated.

$$m_l c_{pl} \frac{dT_l}{dt} = \frac{\lambda_{CH}}{dr}\left(S_{l-1}(T_{l-1} - T_l) + S_l(T_{l+1} - T_l)\right) - Q_l \quad (1)$$

$$Q_l = N_{w,l} \frac{\lambda_{CH}}{r_w} S_{w,l}(T_l - T_{w,l}) \quad (2)$$

The hypothesis of no convection inside the emulsion droplet is adopted. This hypothesis is made by numerous authors such as Sazhin [7] and Jacques [14] considering Heavy Fuel-Oil as viscous enough to prevent internal circulation. This is especially relevant for heavy fuels because of their higher viscosity in comparison with lighter ones such as diesel or kerosene [1]. Hence, only conductive heat transfer is modeled across the surface areas S_l between the sphere layers. Eq. (2) also holds this hypothesis, because it takes conduction into account at the surface of the internal water droplets. A rapid calculation gives a thermal conductivity of emulsified fuel (water vol. fraction 0.1 and internal droplets diameter 10 μm) 7% higher than pure fuel, while uncertainty of thermal conductivity is about 10% due to various provenances of Heavy Fuel-Oil. As a consequence, thermal conductivity is given a higher value for pure Heavy Fuel-Oil (Table 1).

This heat transfer to internal water droplets enables to determine their temperature and thermal expansion. As explained later, the onset and the expansion in volume of micro-explosion are directly linked to the temperature of internal water droplets. And a correct value of the heat capacity of water is crucial to determine their instantaneous temperature. Fig. 2 shows the specific heat of water $c_{p,w}$ as temperature-dependent. Its values in the liquid metastable domain are issued from the data of Cahn [15].

Eq. (3) is the correlation of Ranz and Marshall [16] giving the convective coefficient α. It enables the account of the relative velocity of the gaseous phase, through the Reynolds number of the droplet Re. It expresses a convective heat transfer depending on the thermo-physical properties of the gaseous

phase through the calculation of the Reynolds and Prandtl numbers. Eq. (3) is applied to the surface of the emulsion droplet, where only convective heat transfer from the gaseous phase is considered. The hypothesis consisting of no radiative heat transfer is one of the major assumptions of the D^2-law theory [17] and is also considered by Sirignano [18,19] in models of burning droplets of fuel.

$$Nu = 2 + 0.6\,Re^{1/2}\,Pr^{1/3} \tag{3}$$

Eq. (4) shows the calculation of the film temperature and the gaseous molar fraction of fuel, following the One-third rule [20,21]. The One-third rule is recommended by Yuen and Chen [22], and is used by Sirignano [19] and Lebouché [23] in models of burning droplets of fuel.

$$T_{\text{film}} = \frac{2T_{\text{ext}} + T_{\text{G}}}{3}, \qquad Y_{\text{film}} = \frac{2Y_{\text{ext}} + Y_{\infty}}{3} \tag{4}$$

Eq. (5) is the gradient applied between the two superficial layers (indiced as ext and ext − 1) as a boundary condition. The conductive heat transfer inside the droplet and the loss of latent heat at its surface are both taken into account. According to Sirignano [18], these two phenomena (e.g. transient liquid heating and droplet vaporisation) exert mutual influence on droplet temperature.

Eq. (5) enables the balance between them to be calculated. Although they require large amounts of energy, the heating and vaporization of water are not accounted for at the droplet surface. The reason for that is the diameter of internal water droplets being equal to the layer thickness in further validations. Indeed, at the surface this thickness is decreasing due to vaporisation, so water is exposed to the gaseous phase. Eq. (2) is then irrelevant, and the internal water droplets of the superficial layer receive a significant heat transfer directly from the gaseous phase, or break up their metastable state and vaporise directly in the gaseous phase. Eq. (5) includes the thickness of the superficial layer dr_{ext}: Contrary to thermally-expanding inside layers in Eq. (1), dr_{ext} decreases because of the surface layer depleting by vaporisation. Thus, dr_{ext} decreases until tiny values, putting computations at risk of divergence.

$$\frac{\lambda_{\text{CH}}}{dr_{\text{ext}}} S_{\text{ext}-1}(T_{\text{ext}} - T_{\text{ext}-1}) = S_{\text{ext}}\alpha(T_{\text{G}} - T_{\text{ext}}) - L_{\text{CH}} W_{\text{VAP}} \tag{5}$$

Eq. (6) holds two criteria of critical thicknesses that are used in this model:

$$dr_{l=\text{ext}} \leqslant \beta dr_{l=\text{ext},t=0} \tag{6}$$

The first one is relative to heat transfer when verified with $\beta = 0.1$. Then Eq. (5) has $\lambda_{\text{CH}}/dr_{\text{ext}}$ replaced by $2\lambda_{\text{CH}}/dr_{\text{ext},t=0}$. This means that the thermal resistance of the superficial layer is neglected, so conduction until the half thickness of the under-surface layer (ext − 1) is considered. The second criterion is concerning vaporisation. Eq. (6) verified with $\beta = 0.01$ enables the remaining liquid fuel to be considered as instantly depleted, then the under-surface layer is becoming the superficial layer.

Eq. (7) expresses the spinodal limit temperature which is the upper boundary of homogeneous nucleation temperature, as expressed by Law [11]. To ensure the possibility of homogeneous nucleation for water, the fuel must have its boiling point above or equal to the spinodal limit temperature of water which is 600 K.

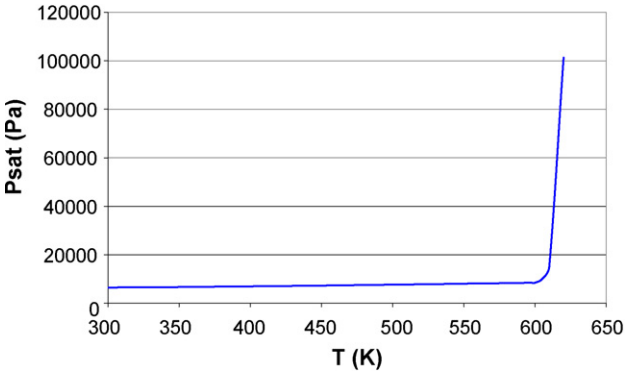

Fig. 3. Assumption of saturation pressure for Heavy Fuel.

$$\left(\frac{\partial P}{\partial V}\right)_T = 0 \tag{7}$$

Fig. 3 shows a value of 620 K for the boiling point of modeled Heavy Fuel-Oil. Hence, just diffusive vaporisation of fuel at the droplet surface is considered, without boiling. Fig. 3 explains the assumption made for the saturation pressure of Heavy Fuel-Oil that reaches atmospheric pressure at 620 K, and holds a low level (<10.000 Pa) below 600 K to generate a slow diffusive vaporisation, hence a substantial increasing in temperature (cf. Eq. (5)). This assumption of saturation pressure results from a hydrocarbon mixture (from C_5 to C_{25}), similar to the Fuel-Oil No. 6 used by Gollahalli [13] in his experiments. However, a difficulty here is that saturation pressure is not precisely mentioned among Heavy Fuel-Oil properties, and a test for the influence of its magnitude on final results is made in this paper.

Eq. (8) expresses the mass flux of fuel W_{vap} calculated at the surface of the emulsion droplet, which is crucial to determine the quantity of fuel provided to the diffusion flame. Kryukov [24] considers the hypothesis of always saturated fuel vapor in the vicinity of the droplet surface, in the case of pure diesel fuel. This hypothesis is also one of the major assumptions made by Law [17] in his summarized D^2-law theory.

$$W_{\text{vap}} = M_{\text{CH}} K S_{\text{p}} \left(\frac{P_{\text{sat,CH}}(T_{\text{ext}})}{R T_{\text{ext}}} - C_{\infty} \right) \tag{8}$$

Eqs. (9) and (10) are used to calculate the mass transfer coefficient K, taking into account the relative velocity, and the thermo-physical properties at every step of time. The mass diffusion coefficient k_C enables to determine K through Nusselt correlation (Eq. (9) [16]). Eq. (10) shows the multicomponent gas-phase diffusion of Wilke [25] used to calculate k_C. The correlation of Wilke is used to take into account the presence of steam in the vicinity of the emulsion droplet. Moreover, mass diffusion coefficients $k_{\text{CH,air}}$ and $k_{\text{w,air}}$ are temperature-dependent. Since $k_{\text{CH,air}}$ is not accurately characterized as an experimental condition, a test for the influence of its magnitude on final results is also carried out in this paper.

$$\frac{K r_d}{k_C} = 1 + 0.3\,Re_{\text{d}}^{1/2}\,Sc_{\text{d}}^{1/3} \tag{9}$$

Table 2
Reference case of micro-explosion experiment by Gollahalli [13]

Environment temperature (K)	1400
Initial emulsion droplet temperature (K)	300
Initial radius of emulsion droplet (μm)	500
Initial radius of internal water droplet (μm)	5
Water weight fraction	0.1
Relative velocity of gaseous phase vs. emulsion droplet ($m\,s^{-1}$)	5
Emulsified fuel	Heavy Fuel-Oil No. 6
Measured micro-explosion delay (ms)	250

$$k_C = \frac{1}{Y_{CH}/k_{CH,air} + Y_w/k_{w,air}} \tag{10}$$

According to Law [26], the hypothesis enabling micro-explosion consists of internal water droplets not moving inside the emulsion, which is called the "Frozen limit". In other words, the hypothesis of "Frozen limit" means no circulation of fluids, as previously explained about the hypothesis of no convection inside the emulsion droplet. In the present study, water and fuel are assumed to vaporise in the same proportion as their initial ratio in the liquid phase ("frozen limit-steady depletion" hypothesis [26]). This assumption leads to take into account the saturation pressure of the most abundant component, which is, in our case of emulsion, the Heavy Fuel-Oil. Eqs. (8), (9) and (10) constitute the diffusive vaporisation considered for the Heavy Fuel-Oil. Eq. (11) expresses the mass of vaporized water dm_w, determined from the hypothesis of steady depletion, where f is the mass fraction of water in the emulsion.

$$dm_w = f \times (dm_{CH} + dm_w) \tag{11}$$

2.2. Validation tests

Results are obtained through an explicit finite-differences method, forward in time and centered in space. Due to the relatively low number of sphere layers (order of magnitude between 10 and 100), the influence of time and space steps on the results of the sphere layers model is properly checked. The relaxation time of particles responsible for conduction of heat are: 10^{-11} s (phonons), 10^{-13} s (electrons). Consequently, 10^{-6} s is a lower limit for the time step in this model. Negligible differences (less than 1) in the vaporisation rate and in the time needed to reach $T_{w,ext-1} = 600$ K are observed in the reference case (cf. Table 2) using a time step of 6.5×10^{-5} s or 4.3×10^{-5} s. The larger value of 6.5×10^{-5} s is used in the further simulations.

All the phenomena influencing the micro-explosion delay (vaporisation and boiling rates, heat transfer to dispersed phase, etc.) are greatly influenced or directly governed by the temperature of Heavy Fuel-Oil. Thus, a special care is taken to validate conductive heat transfer across the emulsion droplet, without the presence of internal water droplets. Eq. (12) represents the analytical conductive heat transfer within a sphere [14]. Its results are compared to results from the sphere layers model in order to validate heat transfer within pure fuel.

$$\rho C_p \frac{dT}{dt} = \lambda_{CH}\left(\frac{\partial^2 T}{\partial t^2} + \frac{2}{r}\frac{\partial T}{\partial t}\right) \tag{12}$$

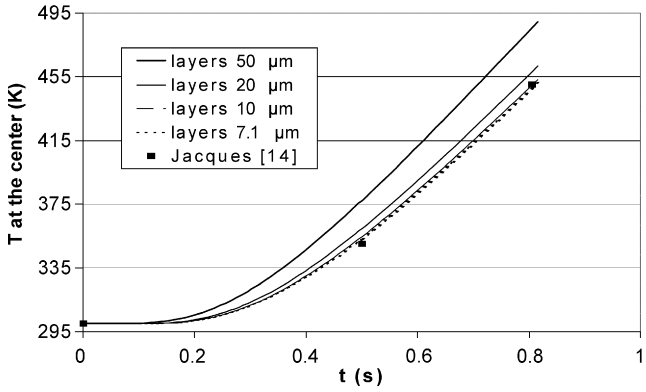

Fig. 4. Influence of sphere layers thickness faced with the analytical result.

Table 3
Test for space step (sphere layers thickness)

Sphere layers model (ref. case Table 2) with $R_w = 2.5$ μm		$t(T_{w,ext-1} = 600$ K) (ms) (Fig. 7)	Vaporization rate ($mm^2\,s^{-1}$) between 0 and 200 ms
Δr	9.1 μm	249.9	0.11
	7.1 μm	248.2	0.11
	5 μm	253.2	0.11

Fig. 4 shows the temperature at the center of a 1 mm diameter pure oil droplet, both calculated analytically and by the sphere layers model, using exactly the same thermo-physical properties and known heat flux imposed at the external surface. The influence of decreasing the sphere layer thickness can be noticed as a convergence reached for 10 μm. Table 3 exposes a test for the space step, with a time step of 6.5×10^{-5} s, where small variation (5 ms) is noticed. Space step (i.e. sphere layer thickness) is ensured to be large enough to enable modelisation of conduction using Fourier's law. Therefore, the space step is fixed at 10 μm in the further simulations.

Fig. 5 shows the first expected result from the sphere layers model, which is the radial distribution of temperature of internal water droplets through the time. Vertical arrows show the surface regressing due to evaporation, i.e. the discretized radial distribution of temperature ending closer and closer to the center. As soon as 113 ms, one can notice that a large part (>60%) of the emulsion liquid water is in metastable state, hotter than 373.15 K.

Thermal expansion of fuel and water, and vaporisation result in variation of the radius of the emulsion droplet through the time. Fig. 6 shows the decreasing of the squared radius of the emulsion droplet through the time. In the present simulations the expansion is not enough to cause an initial increase of the radius against vaporisation. Thus the internal velocity created by expanding liquids result as negligible in the further validation cases. The calculations are stopped at 251 ms. Over the first 250 ms, the squared radius r_d^2 decreases as a linear function of time, as it is thoroughly seen in the literature [6,14,15,27,28].

Numerous authors, as Law [7,14,17] consider a constant vaporisation rate, expressing the linear decreasing of the squared diameter of the droplet through the time. This is included in the already mentioned D^2-law [17]. Tables 3 and 4 report va-

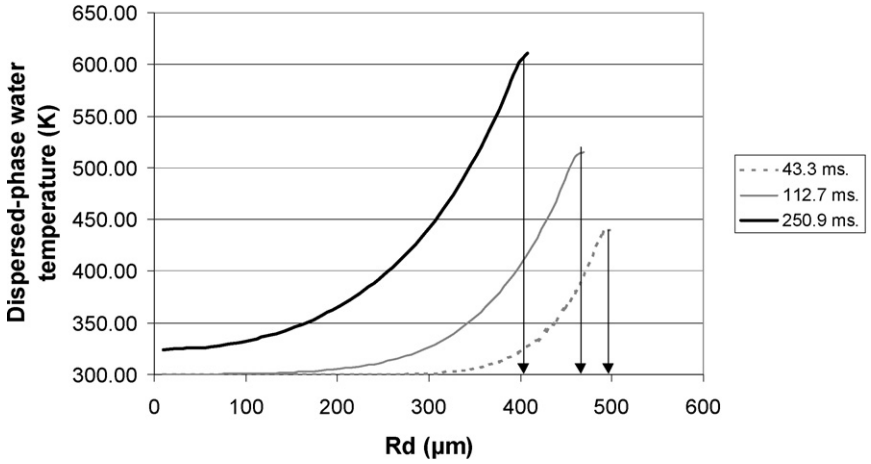

Fig. 5. Radial distribution of temperature increasing though the time.

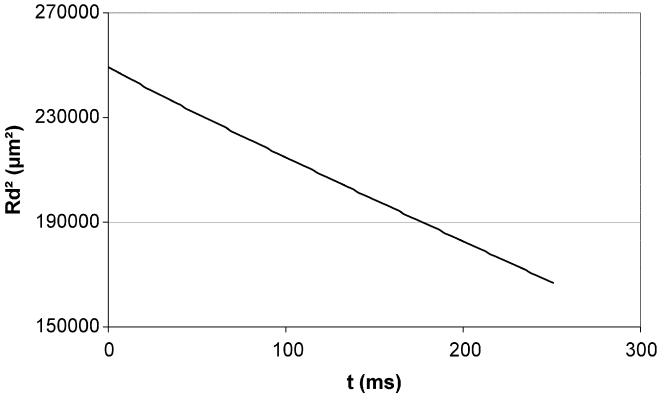

Fig. 6. Decreasing of squared radius through the time in Reference case (cf. Table 2).

Table 4
Evaporation rate with various ambient temperature

Sphere layers model (ref. case Table 2 with various T_∞)		Vaporisation rate ($mm^2\,s^{-1}$) between 0 and 200 ms
T_∞	1000 K	0.06
	1125 K	0.08
	1375 K	0.1
	1500 K	0.12

porisation rates issued from the model. In the vaporisation rates reported, the decreasing of diameter over the first 200 ms is taken into account. The sphere layers model indicates a vaporisation rate as high as 0.14 $mm^2\,s^{-1}$ for the reference case until the predicted micro-explosion delay. This magnitude is in accordance with usual vaporisation rates measured or calculated in the literature for neat heavy fuels (between 0.1 and 1.5 $mm^2\,s^{-1}$). Table 4 shows the influence of ambient temperature on the vaporisation rate: as expected, a faster vaporisation is clearly linked to a higher gaseous flow temperature.

The modelisation of heat transfer results in the increasing temperatures of the surface-layer of fuel (T_{ext}), and of the internal water droplets in the under-surface layer ($T_{w,ext-1}$). Fig. 7 represents these temperatures within successive spherical layers, becoming the surface layer each at their turn. Indeed, every time a surface layer is totally depleted, T_{ext} jumps as the new surface layer is suddenly exposed to convective heat transfer from gaseous phase, and $T_{w,ext-1}$ drops to the colder temperature (~10 K in difference) of the new under-surface layer. Over the whole droplet lifetime the surface temperature is a concave function of time, as can be seen from other models of burning droplets of fuel [27,28]. A thinner space step (i.e. smaller thickness of sphere layer) could partly smooth these numerical jumps. Nevertheless, Eq. (2) does not strictly authorize sphere layers thinner than the diameter of its internal water droplets.

3. Validations of the micro-explosion delay

In this part, using assumption of homogeneous nucleation, the criterion for micro-explosion is analyzed, and the resulting prediction of micro-explosion delay is discussed against experimental validation.

In metastable liquid water, homogeneous nucleation is actually launched at the kinetic limit. Law [11] considers the spinodal limit as an upper approximation of the kinetic limit, following Eberhart [29] that demonstrates the spinodal limit temperature as an excellent correlation with the observed kinetic limit of superheat. When reaching the spinodal limit, a metastable water droplet is surely vaporised. In the case of water, the spinodal limit is between 550 and 600 K [11], because Eq. (13) can use two different equations of state (namely, Van der Waals or Berthelot) for the metastable liquid water, resulting in these two different values [11]. Apfel [30] observed small droplets of liquid metastable water reaching a temperature of 553 K, and greater superheatings under dynamic conditions. To sum up, even if the spinodal limit temperature is not actually reached by the real emulsion, the sphere layers model uses it as a criterion for the launching of homogeneous nucleation. As already mentioned, it is extremely important to realize that this assumption of homogeneous nucleation suits the situation of an alone, unsuspended emulsion droplet in a flow of gas in a so-called "drop tower" facility like the one used in Gollahalli experiments [13] (Fig. 8).

Fig. 4 shows that at any time, the hottest internal water droplets are located under the surface of the emulsion droplet.

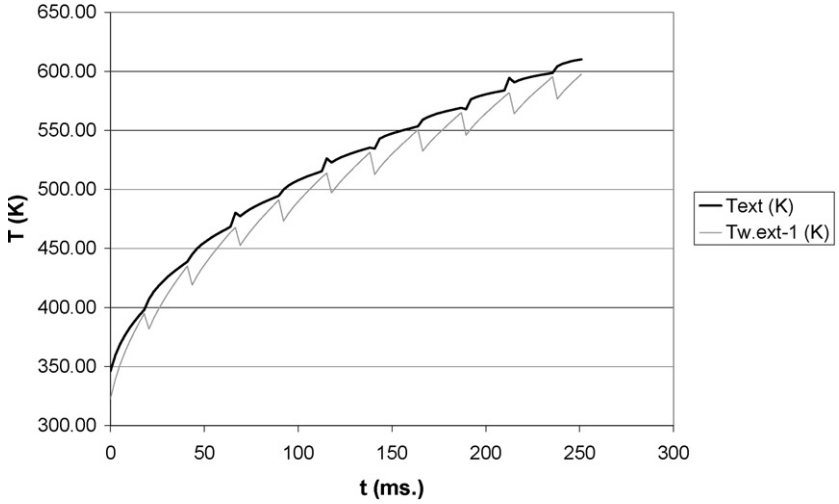

Fig. 7. Increase in temperatures of fuel and water at the surface of the emulsion droplet (cf. ref. case Table 2).

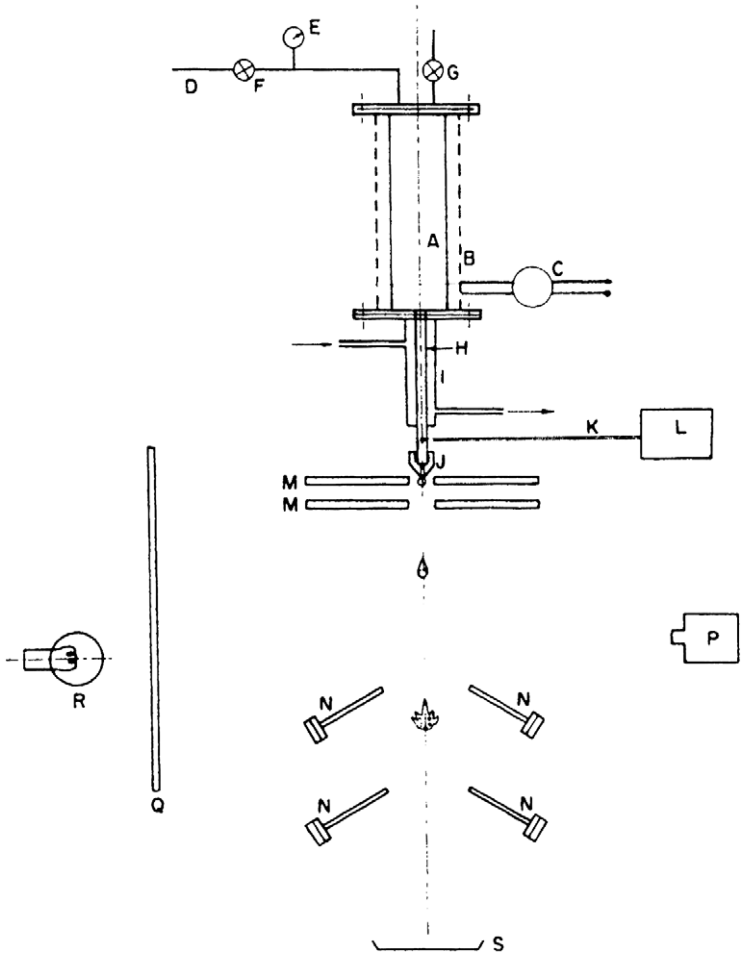

Fig. 8. "Drop tower" facility used by Gollahalli [13].

In this paper, the criterion for micro-explosion consists of these under-surface water droplets reaching the spinodal limit temperature (cf. Eq. (7)). Chen and Wang [12] explain that if micro-explosion effects are localized at the surface, then they may result in the ejection of tiny masses of liquid fuel towards the gaseous environment, without any disintegration inside the emulsion droplet. The criterion for micro-explosion consists of the under-surface metastable water droplets reaching a temperature between 550 and 600 K, and the sphere layers model is used to provide the corresponding range of time throughout its unsteady modelisation. Thus, vaporisation of water droplets not located at the superficial layer (indiced as ext) but within the layers under the superficial one ($ext-1$, $ext-2$, $ext-3$, ...) is considered for the criterion of micro-explosion. In the reference

case (Table 2), this criterion for micro-explosion is reached at 251 ms in the ext − 1 layer, at 281 ms in the ext − 2 layer, and at 323 ms in the ext − 3 layer. The criteria hold at the layers ext − 2 and ext − 3 are rejected because of temperatures over the boiling point reached by the fuel located in the upper layers. Its boiling would put the internal water droplets in contact with fuel vapor, launch nucleation and initiate micro-explosion through another criterion depending exclusively on the boiling point of the fuel. As a consequence, vaporisation of water droplets located not at the superficial layer, but within the layer under the superficial one (ext − 1) is considered to initiate the micro-explosion, at 251 ms in the reference case.

Micro-explosion, which means disintegration of the whole emulsion droplet, is possible if numerous enough water droplets do vaporise altogether in a short laps of time across the emulsion droplet. Concerning that, the underlying hypothesis is the launch of nucleation on a water droplet when in contact with the steam issued from a neighbor water droplet in the emulsion. Hence, the onset of nucleation is propagated deeper and deeper inside the emulsion droplet. This is especially relevant in finely-dispersed emulsion [6] like the one used in Gollahalli experiments ($\sim 10^5$ water droplets enclosed in a 1 mm diameter emulsion droplet). This propagation through the whole emulsion droplet is expected to be shorter than the micro-explosion delay, because the characteristic duration of such a unique and total disintegration of an emulsion droplet is cited as less than 0.2 ms [5,13]. Due to this short characteristic duration of micro-explosion, it is considered as negligible in comparison with the micro-explosion delay.

Fig. 5 indicates that, in the reference case (cf. Table 2), water droplets are in metastable state from a radius of 200 μm to the surface, at the predicted micro-explosion delay. This creates a potential mechanical work of expansion when vaporising at micro-explosion: as considered by Wolfe [27] at breaking up of metastable state, the enthalpy above boiling point compensates for the latent heat of vaporisation, and the mass of liquid water m_w is partly, but fastly vaporized. Eq. (13) expresses m_{steam}, which is this vaporised part of m_w. V_{steam} is the volume of steam created by the sudden vaporisation of metastable water throughout the whole emulsion droplet. It works as an indicator of the potential mechanical work issued from the micro-explosion phenomenon: Eq. (13) is applied to the emulsion droplet in the reference case (cf. Table 2) at the predicted micro-explosion delay (251 ms), supposing simultaneous vaporisation of all the liquid metastable water contained in the emulsion droplet. It results in a created volume of steam of 1.13×10^{-8} m^3 at atmospheric pressure in this case. This volume is 40 times the volume of the emulsion droplet at predicted micro-explosion time, or 22 times the initial volume of the emulsion droplet. This ratio of the created volume of steam to the volume of the emulsion droplet at micro-explosion delay represents an indicator for its potential work of expansion. According to this volume ratio of 40, unique disintegration of the whole emulsion droplet at the same time is supposed, as actually observed in Gollahalli experiments [13].

$$m_{steam} = \frac{m_w C p_w (T_{w,l} - T_{bp,w})}{L_w} \tag{13}$$

Table 5
Test for the influence of thermo-physical properties in the reference case (Table 1)

Thermo-physical property of Heavy Fuel-Oil	Deviation of property (%)	t ($T_{w,ext-1} = 600$ K) (ms)
Latent heat L_f	+10	254
	−10	234
Heat capacity c_p	+10	275
	−10	227
Thermal conductivity λ	+10	252
	−10	236
Saturation pressure P_{sat}	+20	277
	−20	211
Binary diffusion coefficient of fuel vapors $k_{CH,air}$	+30	290
	−30	210

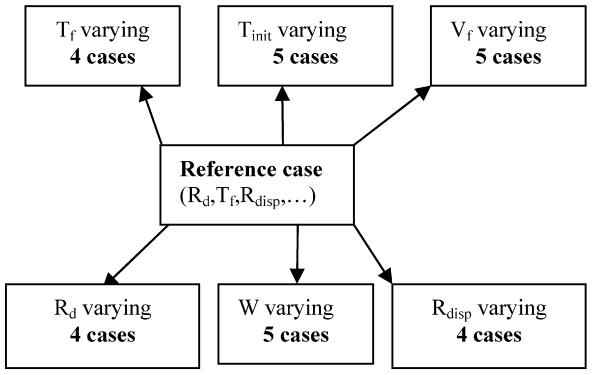

Fig. 9. 27 different sets of parameters differing from the "reference case" tested by Gollahalli [13].

Once a range of time for micro-explosion delay is predicted using this criterion, its dependence to thermo-physical properties of Heavy Fuel-Oil has to be investigated, because the properties of Heavy Fuel-Oil are not strictly defined. Table 5 exposes tests for the criterion of micro-explosion in the reference case, and its sensitivity to realistic ranges of the thermo-physical properties for Heavy Fuel-Oil. Over these ranges, changes in the micro-explosion delay are less than 16%. This reveals a low sensitivity of micro-explosion delay to properties of Heavy Fuel-Oil, despite a large number of equations modeling interconnected phenomena.

Eq. (14) shows an assumption of film temperature different from the one used in the sphere layers model. With this different assumption of film temperature, the criterion of micro-explosion in the reference case is reduced to 234 ms.

$$T_{film} = \frac{T_{ext} + T_G}{2} \tag{14}$$

Once a range of time for micro-explosion delay is predicted using this criterion, a validation remains to be done, using experimental measurements of micro-explosion delays. First, in the reference case, micro-explosion was observed at 250 ms, and the simulation by the sphere layers model reaches the criterion of homogeneous nucleation at 251 ms. Thanks to this accordance, variations from the reference case can also be properly compared between numerical and experimental data.

Fig. 9 exposes the way the different cases were organized. Gollahalli [13] carried out 27 different experiments in order to

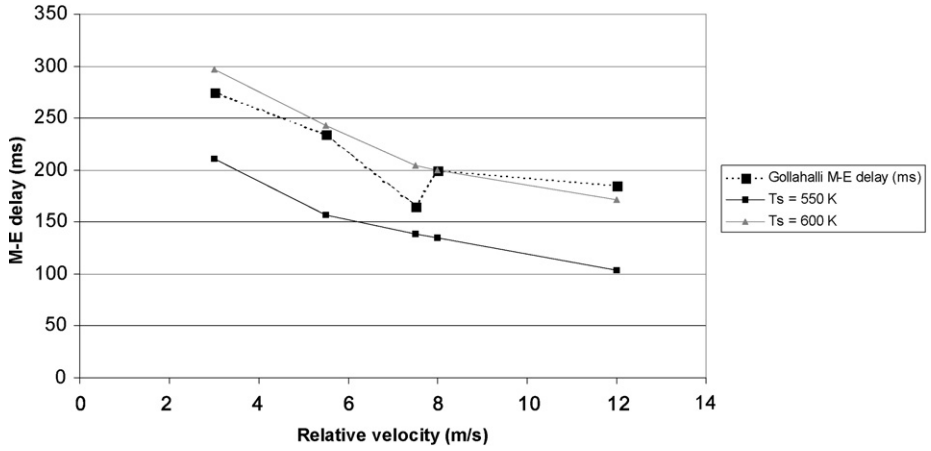

Fig. 10. Comparison between experimental and numerical results with varying relative velocity.

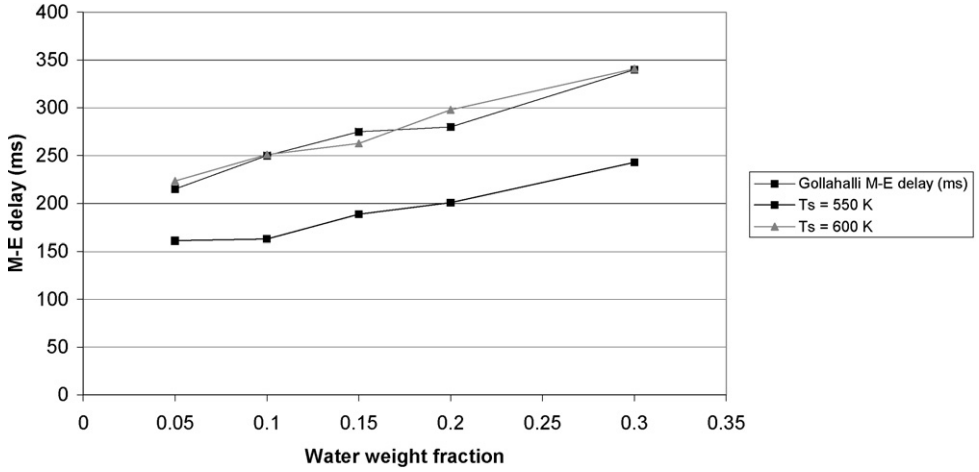

Fig. 11. Comparison between experimental and numerical results with varying water weight fraction.

quantify the influence of individual varying parameters. This means that all of the tested configurations have only one varying parameter from the reference case (cf. Table 2). Such an experimental plan enables to validate separately the influence of each of these combustion parameters on the micro-explosion delay.

The influences of 6 parameters are tested: Initial radius of the emulsion droplet, initial radius of internal water droplets, initial temperature of the emulsion droplet, temperature in the environment gaseous phase, relative velocity of environment gaseous phase vs. emulsion droplet, water weight fraction in the emulsion [13]. Gollahalli [13] uses a gas, burning at the leanest gas/air ratio possible, to create a given temperature in the environment gaseous phase. Micro-explosion delays are measured by counting the movie frames from a camera. As already mentioned, in the experiments of Gollahalli [13], disintegration of emulsion droplet by means of micro-explosion are always seen as sudden and total, without any secondary or tertiary disintegration, as can be seen in other experiments [6]. The emulsion droplets are seen to ignite on photographies in [13]. Due to the relative velocity of the ambient gaseous phase, the diffusion flame is observed as a wake behind the emulsion droplet, its flame front being more than one droplet diameter distant. Hence, a modelisation of a spherical diffusion flame would be irrelevant around the droplet, and the sphere layers model only considers a hot gaseous environment without a surrounding flame.

The experimental micro-explosion delays measured by Gollahalli [13] are faced with the range of homogeneous nucleation issued from the sphere layers model (under-surface water droplets reaching a temperature of 550 and 600 K).

Figs. 10–15 expose these validations. Fig. 10 shows a decrease of micro-explosion delay along with an increasing relative velocity, that is known to increase both the heat transfer and the vaporisation for the emulsion droplet, respectively to heat it and to cool it (Eqs. (3), (5) and (9)). The slope of the predicted micro-explosion delay is in close accordance with the measured one, which is interpreted as a satisfactory balance between the two contradictory thermal influences. Furthermore, the prediction of the upper spinodal limit temperature (600 K) is much more relevant than the lower one (550 K). One can notice the range of tested velocity from 3 to 12 m/s, which is in the lower range of injection velocities in usual atmospheric boilers, where injection velocity can be as high as 50 m/s.

Fig. 11 indicates an increase in the micro-explosion delay along with an increasing water content in the emulsion, with a

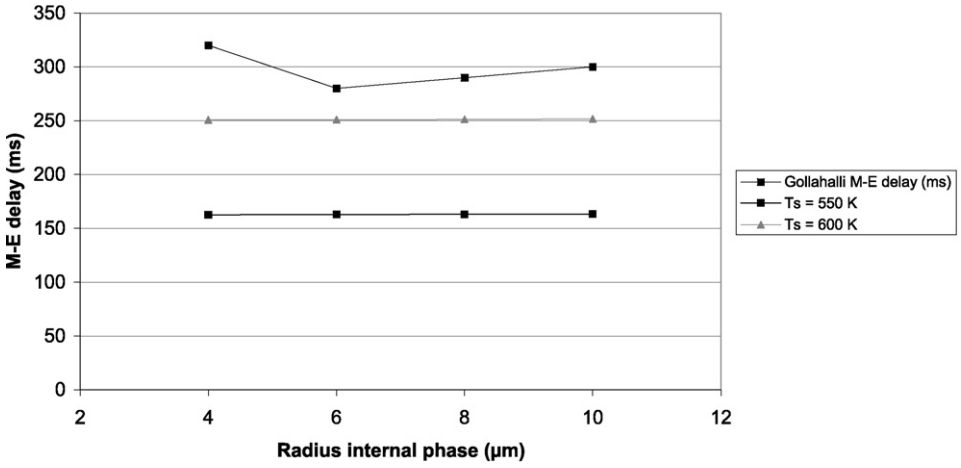

Fig. 12. Comparison between experimental and numerical results with varying radius of internal water droplets.

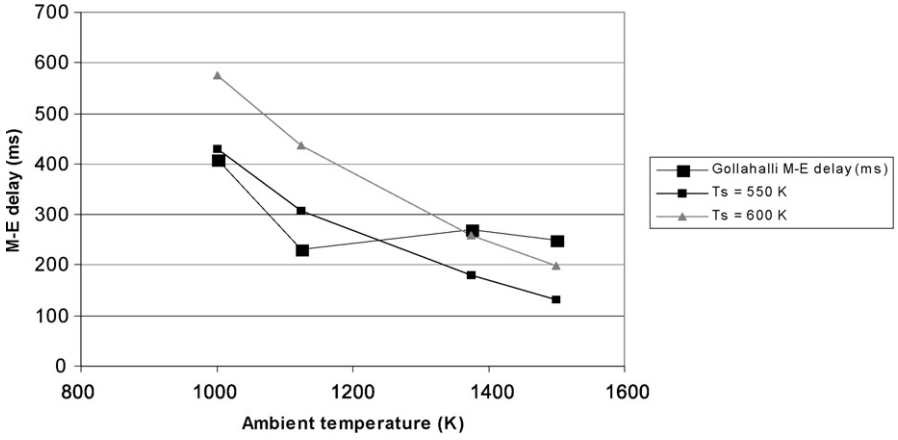

Fig. 13. Comparison between experimental and numerical results with varying ambient temperature.

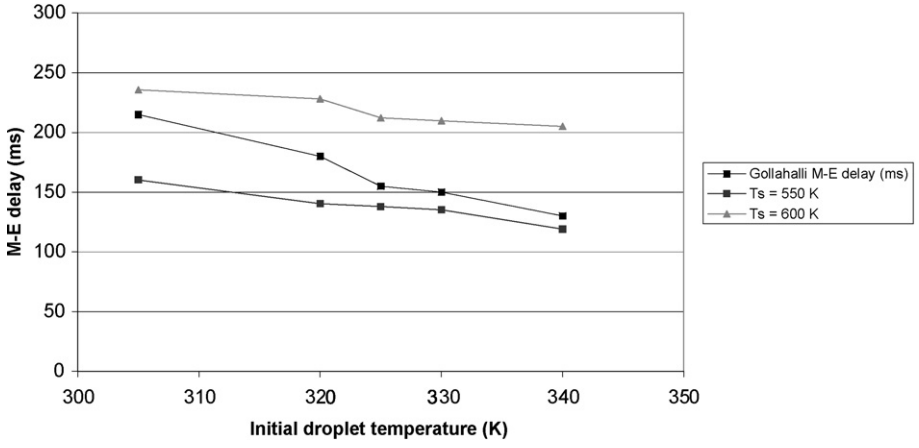

Fig. 14. Comparison between experimental and numerical results with varying initial temperature of emulsion.

remarkable accordance in the slope of the micro-explosion delay, remaining close to the upper spinodal limit temperature. Such an agreement with experimental data reveals the accuracy of Eqs. (9) and (10) applied in the gaseous phase to take the presence of water into account through the diffusion coefficient of steam. The assumption of steady depletion (Eq. (11)), being an essential part of the demonstrated modelisation, is also reinforced by this accordance.

Fig. 12 exposes the validation with varying radius of internal water droplets. In three cases, the internal water droplets are larger than layer thickness: they are considered as entirely enclosed inside the layer containing their center. A decay of <50 ms is observed in all the cases tested. 3 cases close to the reference case (radius of water droplets: 5 µm) are measured between 200 and 250 ms, which rises the question of an experimental offset. Variations in micro-explosion delay due

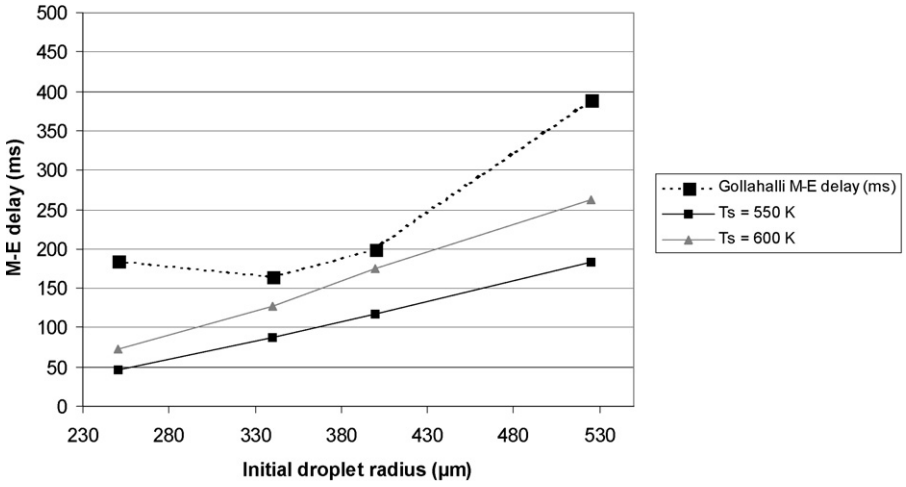

Fig. 15. Comparison between experimental and numerical results with varying initial radius of emulsion droplet.

to changes in diameter of internal water droplets are not large in amplitude (less than 30 ms). Nevertheless, the experimental results show a slight minimum of micro-explosion delay at a radius of 6 μm. Such an optimum could be of a high importance to owners of emulsion-burning facilities, that are searching for the optimal way to disperse the water in the emulsion. One satisfactory point is that the non-sensitivity of the micro explosion delay to such a dramatic increase of the heat-exchanging surface towards inside water droplets is displayed by both the experimental and the numerical results. This is interpreted as the temperatures of heavy fuel and inside water closely following each other, whatever the diameter of inside water droplets (in the considered range of diameter). In fact, in the sphere layers model their temperatures are remaining less than 1 K different all across thermal history of the emulsion droplet.

Fig. 13 shows a longer micro-explosion delay with increasing ambient temperature, as also observed in drop-tower experiments by Chen and Wang [12]. At an ambient temperature of 1000 K, the predicted micro-explosion delay is reached slightly before the lower spinodal limit temperature, and slightly after the upper one at 1375 K and 1500 K, indicating a different slope between numerical prediction and measurement. Due to an ambient temperature controlled by means of natural gas combustion in the experiments of Gollahalli [13], the range of adiabatic flame temperature for liquid fuels could not be explored over 1500 K.

Fig. 14 shows the validation with varying initial temperature of the emulsion droplet. The results show good agreement. At lower initial temperature, micro-explosion happens when T_s reaches the higher limit of spinodal temperature range (600 K), and vice versa. Fig. 13 also exhibits this difference between upper and lower spinodal limit, along with ambient temperature. To sum up, with a varying initial or ambient temperature the slope of the micro-explosion delay along with these temperatures differs between its experimental measurement and its numerical prediction. These differences between numerical and experimental slopes can be interpreted as follows according to Figs. 13 and 14: The higher the heat transfer, the higher the boundary of spinodal limit; and vice versa.

Fig. 15 exposes the validation with varying initial radius of the emulsion droplet. Once more, 3 cases close to the reference case (500 μm) are measured 3 times between 200 and 250 ms. This puts the experimental result for 530 μm (390 ms) at question. Also, for an initial radius of 230 μm, complete evaporation is reached before 150 ms according to the sphere layers model. Nevertheless, the overall trends agree for a decrease of micro-explosion delay along with a decreasing initial radius of emulsion droplet. However, the slopes of the micro-explosion delay show a different behavior in the domain of initial radius tested, with a minimum at a radius of app. 350 μm for experimental data and a constant increase for numerical results.

For each of the 27 tested cases, the deviation between experimental micro-explosion delays and numerical boundaries issued from the criterion of micro explosion is calculated. This deviation is considered as null if the experimental micro-explosion delay is between the boundaries of our criterion. If not, the deviation is the gap between the experimental micro-explosion delay, and its closer boundary of our criterion. Thus, the average gap over the 27 tested cases is less than 25 ms, with experimental micro-explosion delays between 200 and 450 ms. Although there are only 27 validation cases, a statistical test show that 70% of the cases show a gap inferior to its standard deviation, which indicates a Gaussian distribution centered over null deviation.

4. Conclusion

In this paper, a validated model of heat and mass transfers acting at the surface and inside an emulsion droplet is presented, including a criterion for the onset of micro-explosion. This sphere layers model results in longer micro-explosion delays with increasing water content and radius of emulsion droplet, and in shorter delays with increasing liquid or ambient temperature, and relative velocity. A validation of micro-explosion delays in 27 different situations has been performed to determine the accuracy of the homogeneous nucleation assumption for the onset of micro-explosion. A discussion about the relevance of the higher (600 K) or the lower (550 K) boundary of

spinodal limit can also start from comparisons in the numerical and experimental slopes of the micro explosion delay along with ambient temperature, and initial temperature of the emulsion droplet.

The low average deviation (25 ms) shows the agreement between numerical range for micro-explosion delay under assumption of homogeneous nucleation, and experimental delay in "drop tower" combustion facility, even with 10 or 30% in properties varying of Heavy Fuel-Oil. Thus, in the situation of an alone and unsuspended emulsion droplet in a flow of gas, the onset of micro-explosion is confirmed to happen at a temperature close to the upper limit for homogeneous nucleation.

Future works will build an extension of this criterion, taking into account heterogeneous nucleation in situations closer to actual furnace situations, and coalescence of internal water droplets in the emulsion.

References

[1] R. Ocampo-Barrera, R. Villasenor, A. Diego-Marin, An experimental study of the effect of water content on combustion of heavy fuel-oil/water emulsion droplets, Combust. Flame 126 (2001) 1845–1855.
[2] N.J. Marrone, I.M. Kennedy, F.L. Dryer, Coke formation in the combustion of isolated heavy oil droplets, Combust. Sci. Tech. 36 (1984) 149–170.
[3] S.R. Gollahalli, M.K. Nasrullah, J.H. Bhashi, Combustion and emission characteristics of burning sprays of a residual oil and its emulsions with water, Combust. Flame 55 (1984) 93–103.
[4] W.B. Fu, L.Y. Hou, L. Wang, F.H. Ma, A study on ignition characteristics of emulsified oil containing flamable fuel, Fuel Proc. Tech. 79 (2002) 107–119.
[5] J.C. Lasheras, A.C. Fernandez-Perello, F.L. Dryer, Experimental observations on the disruptive combustion of free droplets of multicomponent fuels, Combust. Sci. Tech. 21 (1979) 1–14.
[6] V.M. Ivanov, P.I. Nefedov, Experimental investigation of the combustion process of natural and emulsified liquid fuels, Trudy Goryachikh Iskopayemykh. 19 (1962) 35–45.
[7] S.S. Sazhin, Bubble nucleation mechanisms of liquid drops superheated in other liquids, Int. J. Heat Mass Trans. 47 (2004) 2927–2940.
[8] F.L. Dryer, Water addition to practical combustion systems – concepts and application, NTIS Report No. DE82021289.
[9] J.M. Ballester, N. Fueyo, C. Dopazo, Combustion characteristics of heavy oil-water emulsions, Fuel 75 (1996) 695–705.
[10] H. Jahani, S.R. Gollahalli, Characteristics of burning Jet A fuel and Jet A fuel-water emulsion sprays, Combust. Flame 37 (1980) 145–154.
[11] C.K. Law, A model for the combustion of oil/water emulsion droplets, Combust. Sci. Tech. 17 (1977) 29–38.
[12] J.T. Chen, C.H. Wang, An experimental investigation of the burning characteristics of water–oil emulsions, Int. Comm. Heat Mass Transfer 23 (1996) 823–834.
[13] S.R. Gollahalli, An experimental study of the combustion of unsupported drops of residual oils and emulsions, Combust. Sci. Tech. 19 (1979) 245–250.
[14] M.T. Jacques, Transient heating of an emulsified water-in-oil droplet, Combust. Flame 29 (1977) 77–85.
[15] R.W. Cahn, Metastable States of Water, Encyclopedia of Material Science and Engineering, Pergammon Press, 1988.
[16] W.E. Ranz, W.R. Marshall Jr., Evaporation from drops, Chem. Eng. Proc. 48 (1952) 141–180.
[17] C.K. Law, Recent advances in droplet vaporization and combustion, Prog. Energ. Combust. Science 8 (1982) 171–201.
[18] W.A. Sirignano, B. Abramzon, Droplet vaporization model for spray combustion calculations, Int. J. Heat Mass Trans. 32 (1989) 1605–1618.
[19] W.A. Sirignano, Fuel droplet vaporisation and spray combustion theory, Prog. Energ. Combust. Sci. 9 (1983) 291–332.
[20] E.M. Sparrow, J.L. Gregg, Evaporation of diesel fuel droplets and classical combustion, Trans. ASME 80 (1958) 879–886.
[21] G.L. Hubbard, V.E. Denny, A.F. Mills, Int J. Heat Mass Trans. 16 (1973) 1003–1008.
[22] M.C. Yuen, N.W. Chen, On drag of evaporating liquid droplets, Combust. Sci. Tech. 14 (1976) 147–154.
[23] G. Castanet, P. Lavieille, F. Lemoine, M. Lebouché, A. Atthasit, Y. Biscos, G. Lavergne, Evaporating budget on an evaporative monodisperse droplet stream using combined optical methods – evaluation of the convective heat transfer, Int. J. Heat Mass Trans. 16 (1973) 1003–1008.
[24] A.P. Kryukov, V.Y. Levashov, S.S. Sazhin, Evaporation of diesel fuel droplets: Kinetic versus hydrodynamic models, Int. J. Heat Mass Trans. 47 (2004) 2541–2549.
[25] C.R. Wilke, Chem. Eng. Prog. 46 (1950) 95–105.
[26] C.K. Law, C.H. Lee, N. Srinivasan, Combustion characteristics of water-in-oil emulsion droplets, Combust. Flame 37 (1980) 125–143.
[27] J. Wolfe, Superheating and microwave ovens, some notes by, School of physics, The University of New South Wales, Sydney. http://www.phys.unsw.edu.au/~jw/superheating.html.
[28] S.S. Sazhin, W.A. Abdelghaffar, E.M. Sazhina, M.R. Heikal, Models for transient droplet heating: Effects on droplet evaporation, ignition, and break-up, Int. J. Therm. Sci. 44 (2005) 610–622.
[29] J.G. Eberhart, H.C. Schnyders, Application of the mechanical stability condition to the prediction of the limit of superheat for normal alkanes, ether, and water, J. Phys. Chem. 77 (1973) 2730.
[30] R.E. Apfel, Vapor cavity formation in liquids, Nature Phys. Sci. 238, 63–64.